Application of the Fast Multipole Method to Hybrid Finite Element–Boundary Element Models ⋆

R. V. Sabariego *, J. Gyselinck, C. Geuzaine, P. Dular [1], W. Legros

Dept. of Electrical Engineering (ELAP), Institut Montefiore, University of Liège Sart Tilman Campus, Building B28, B-4000 Liège, Belgium

Abstract

This paper focuses on the acceleration of the hybrid finite element – boundary element analysis of 2D eddy current problems by means of the fast multipole method. An adaptive truncation scheme for the expansion of the 2D Laplace Green function is proposed. A linear time harmonic test case is considered. The results obtained with the hybrid model, with and without fast multipole acceleration, agree well with those obtained with a finite element model. The computational cost of the three calculations is compared and discussed. The proposed adaptive truncation scheme significantly contributes to the computation time savings achieved with the fast multipole method, particularly when dealing with moderate sized problems.

Key words: fast multipole method, finite element method, boundary element method, hybrid method, Laplace function

1 Introduction

Hybrid finite element – boundary element (FE-BE) models are particularly suited for solving open electromagnetic field problems that comprise nonlinear media and movement [3]. They are extensively used for quasi-stationary and scattering problems.

The BE part of the hybrid FE-BE technique generates dense blocks in the system matrix and significantly limits the size of the problem to be handled,

⋆ The research was carried out in the frame of the Inter-University Attraction Poles for fundamental research funded by the Belgian government.

* Corresponding author.
Email address: R.Sabariego@ulg.ac.be (R. V. Sabariego).

[1] P. Dular is a Research Associate with the Belgian National Fund for Scientific Research (F.N.R.S.)

in particular for 3D problems [2]. The fast multipole method (FMM) [7] can be employed to overcome this limitation. This mathematical tool, which is applied in conjunction with an iterative solver, e.g. GMRES [8], speeds up the matrix-vector multiplications in every iteration and reduces the computational cost and the memory requirements.

The FMM has been successfully applied to BE models in both high frequency [9] and low frequency problems [2]. With regard to hybrid FE-BE models, the FMM has been solely used in scattering applications [5]. This paper deals with the resolution of a hybrid FE-BE model in low frequency accelerated by the FMM. A 2D eddy current test case is discussed in detail.

2 Hybrid FE-BE model for a 2D eddy current problem

A time harmonic eddy current problem in $\mathbb{R}^2$ is considered. The FE method is used in a domain Ω, the boundary of which is denoted Γ. It comprises a domain Ω_s^{in} and a domain Ω_c (with conductivity σ) in which eddy currents may appear. The BE method accounts for the free space exterior to Ω extending to infinity and a domain Ω_s^{ext}. A current density $\underline{j} = j_s(x,y)\,\underline{1}_z$, directed along the z-axis, is given in the domains Ω_s^{in} and Ω_s^{ext}. The rest of the exterior domain is current free. The FE part Ω and the BE part Γ of the hybrid model are discretised with e.g. triangular elements and straight line segments, respectively.

The present analysis is restricted to the linear time harmonic case, though it can be easily extended to the nonlinear case and the transient case. The complex notation is adopted for denoting the sinusoidal time variation of frequency f and pulsation $\omega = 2\pi f$. The imaginary number is denoted $\imath$.

The governing differential equations and constitutive laws are

$$\operatorname{curl} \underline{h} = \underline{j}\,, \quad \operatorname{div} \underline{b} = 0 \quad \text{and} \quad \underline{h} = \nu\,\underline{b} \qquad \text{in } \mathbb{R}^2\,, \tag{1}$$

$$\operatorname{curl} \underline{e} = -\imath\,\omega\,\underline{b} \quad \text{and} \quad \underline{j} = \sigma\,\underline{e} \qquad \text{in } \Omega_c\,, \tag{2}$$

where the z-component of the magnetic field $\underline{h}(x,y)$ and the magnetic induction $\underline{b}(x,y)$ vanish, the current density $\underline{j}$ and the electric field $\underline{e}$ are directed along the z-axis, and the magnetic reluctivity ν and the electrical conductivity σ are constant scalars.

The eddy current problem is formulated in terms of the magnetic vector potential $\underline{a} = a(x,y)\,\underline{1}_z$ in Ω and the equivalent current layer $\underline{q} = q(\xi)\,\underline{1}_z$ on Γ [6,4]. For any continuous potential a, (1b) and (2a) are fullfilled on account of

$$\underline{b} = \operatorname{curl} \underline{a} = \underline{1}_z \times \operatorname{grad} a \quad \text{and} \quad \underline{e} = -\imath\,\omega\,\underline{a} + \operatorname{grad} v\,. \tag{3}$$

where v is the electric scalar potential. In absence of external voltage sources, the term $\operatorname{grad} v$ in (3b) can be omitted.

From $\operatorname{curl} \underline{h} = -\operatorname{div}(\nu \operatorname{grad} a)\,\underline{1}_z$, it follows that the weak form of Ampère's

law (1a) in Ω is given by

$$\int_\Omega \nu \, \mathrm{grad}\, a \cdot \mathrm{grad}\, a' \, \mathrm{d}\Omega + \imath\, \omega \int_{\Omega_c} \sigma \, a \, a' \, \mathrm{d}\Omega \;=\; \int_{\Omega_s^{in}} j_s \, a' \, \mathrm{d}\Omega + \oint_\Gamma \nu \frac{\partial a}{\partial n} \, a' \, \mathrm{d}\Gamma \,, \quad (4)$$

where the test function $a'(x, y)$ is continuous in Ω.

The BE model is coupled through the contour integral in (4) of the product of the test function a' and the tangential magnetic field on Γ, $h_t = \nu b_t = \nu \frac{\partial a}{\partial n} = \nu \, \underline{n} \cdot \mathrm{grad}\, a$, where $\underline{n}$ is the unit normal vector on Γ pointing into Ω. Indeed, the potential a in $\mathbb{R}^2 \backslash \Omega$ can be expressed in terms of the equivalent current layer $q(\xi)$ on Γ and the given current density $j_s(x, y)$ in Ω_s^{ext}:

$$a = \frac{1}{\nu_0} \oint_\Gamma q \, G \, \mathrm{d}\Gamma + \frac{1}{\nu_0} \int_{\Omega_s^{ext}} j_s \, G \, \mathrm{d}\Omega \quad \text{with} \quad G = -\frac{1}{2\pi} \ln r \;, \quad (5)$$

and r the distance from a source point on Γ to an observation point in $\mathbb{R}^2 \backslash \Omega$.

Further, from (5) it follows that the tangential magnetic field on the boundary Γ is given by

$$\nu \frac{\partial a}{\partial n} = \frac{1}{2} q + \oint_\Gamma q \, \frac{\partial G}{\partial n} \, \mathrm{d}\Gamma \; + \int_{\Omega_s^{ext}} j_s \frac{\partial G}{\partial n} \, \mathrm{d}\Omega \,. \quad (6)$$

On the basis of the discretisation of Ω and Γ, $\#a$ real basis functions $\alpha_j(x, y)$ and $\#q$ real basis functions $\beta_l(\xi)$ are defined for the vector potential $a(x, y)$ and the equivalent current layer $q(\xi)$, respectively:

$$a(x, y) = \sum\nolimits_{j=1}^{\#a} a_j \, \alpha_j(x, y) \quad \text{and} \quad q(\xi) = \sum\nolimits_{l=1}^{\#q} q_l \, \beta_l(\xi) \,. \quad (7)$$

The complex coefficients a_j and q_l are assembled in the column matrices $\boldsymbol{A}$ and $\boldsymbol{Q}$.

By employing the $\#a$ basis functions $\alpha_i(x, y)$ as test functions in the weak form (4a) and considering (6), a system of $\#a$ complex algebraic equations is obtained. The equation (5) is imposed by weighing it on Γ with the $\#q$ basis functions $\beta_k(\xi)$. The resulting system of $\#a + \#q$ complex equations of the hybrid model can thus be written as:

$$\begin{bmatrix} \boldsymbol{S} + \imath\, \omega \, \boldsymbol{L} & \boldsymbol{C} \\ \boldsymbol{D}^T & \boldsymbol{M} \end{bmatrix} \begin{bmatrix} \boldsymbol{A} \\ \boldsymbol{Q} \end{bmatrix} = \begin{bmatrix} \boldsymbol{J}^{in} + \boldsymbol{J}^{ext} \\ \boldsymbol{K} \end{bmatrix} . \quad (8)$$

$\boldsymbol{S}$ and $\boldsymbol{L}$ are sparse $\#a \times \#a$ FE matrices:

$$S_{i,j} = \int_\Omega \nu \, \mathrm{grad}\, \alpha_i \cdot \mathrm{grad}\, \alpha_j \, \mathrm{d}\Omega \,, \quad L_{i,j} = \int_{\Omega_c} \sigma \, \alpha_i \, \alpha_j \, \mathrm{d}\Omega \,. \quad (9)$$

The partially dense $\#a \times \#q$ matrices $\boldsymbol{C}$ and $\boldsymbol{D}$, and the full $\#q \times \#q$ matrix

$\boldsymbol{M}$ are given by

$$C_{i,l} = \oint_\Gamma \alpha_i \left(\frac{1}{2}\beta_l + \oint_\Gamma \beta_l \frac{\partial G}{\partial n} \, \mathrm{d}\Gamma \right) \mathrm{d}\Gamma \ , \quad D_{j,k} = \oint_\Gamma \alpha_j \beta_k \, \mathrm{d}\Gamma \, , \tag{10}$$

$$\text{and} \quad M_{k,l} = \frac{1}{\nu_0} \oint_\Gamma \beta_k \left(\oint_\Gamma \beta_l \, G \, \mathrm{d}\Gamma \right) \mathrm{d}\Gamma \ . \tag{11}$$

The $\#a \times 1$ column matrices $\boldsymbol{J}^{in}$ and $\boldsymbol{J}^{ext}$ and the $\#q \times 1$ column matrix $\boldsymbol{K}$ follow from the imposed current density in Ω_s^{in} and Ω_s^{ext}:

$$J_i^{in} = \int_{\Omega_s^{in}} j_s \, \alpha_i \, \mathrm{d}\Omega \ , \quad J_i^{ext} = \oint_\Gamma \alpha_i \left(\int_{\Omega_s^{ext}} j_s \frac{\partial G}{\partial n} \, \mathrm{d}\Omega \right) \mathrm{d}\Gamma \ , \tag{12}$$

$$\text{and} \quad K_k = \frac{1}{\nu_0} \oint_\Gamma \beta_k \left(\int_{\Omega_s^{ext}} j_s G \, \mathrm{d}\Omega \right) \mathrm{d}\Gamma \ . \tag{13}$$

Solving the eddy current problem requires the assembly of the system of algebraic equations (8) and its resolution. The assembly of the BE part is expensive, especially when numerical integration is used. If straight line elements and piecewise constant basis functions are used for $q(\xi)$, the inner integrals in (10) and (11) can be evaluated analytically.

3 Fast multipole method

The fast multipole method (FMM) reduces the operational count by spatially decomposing the boundary Γ into $\#g$ groups of elements, $\Gamma = \bigcup_{g=1}^{\#g} \Gamma_g$, and determining the interactions between distant groups by means of the multipole expansion of the Green function. Hereto, for each group a geometrical center is considered. This is illustrated in Fig. 1.

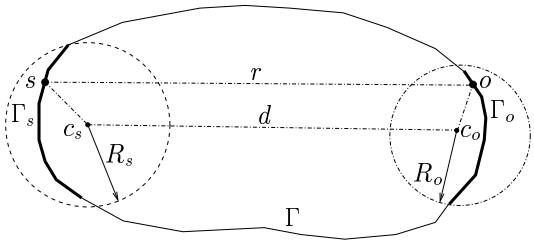

Fig. 1. Distant groups Γ_s and Γ_o on contour Γ, with respective centers c_s and c_o

The simplest way to achieve these groups is to build an octree [2]. Note that in a single level FMM, as described in the present paper, only the finest level of the octree is considered.

3.1 Multipole expansion

For sake of simplicity, points (x, y) in $\mathbb{R}^2$ will be denoted by complex numbers, i.e. $\boldsymbol{z} = x + \imath\, y$. Let $\boldsymbol{z}_s$ be a source point in a given group centered in $\boldsymbol{z}_{sc}$ and

$\boldsymbol{z}_o$ an observation point in a distant group of center $\boldsymbol{z}_{oc}$. Omitting the factor $-1/2\pi$, the 2D Laplace Green function (5b) is then expanded as [7]:

$$\ln r = \Re\Big(\ln(\boldsymbol{z}_o - \boldsymbol{z}_s)\Big) = \Re\left(\sum_{u=0}^{\infty}\sum_{v=0}^{\infty} \mathcal{D}_u\left(\boldsymbol{z}_o, \boldsymbol{z}_{oc}\right) \mathcal{T}_{u,v}\left(\boldsymbol{z}_{oc}, \boldsymbol{z}_{sc}\right) \mathcal{A}_v\left(\boldsymbol{z}_{sc}, \boldsymbol{z}_s\right)\right) \quad \text{with} \tag{14}$$

$$\mathcal{D}_u\left(\boldsymbol{z}_o, \boldsymbol{z}_{oc}\right) = \left(\boldsymbol{z}_{oc} - \boldsymbol{z}_o\right)^u, \qquad \mathcal{A}_v\left(\boldsymbol{z}_{sc}, \boldsymbol{z}_s\right) = \left(\boldsymbol{z}_s - \boldsymbol{z}_{sc}\right)^v, \tag{15}$$

$$\mathcal{T}_{u,v}\left(\boldsymbol{z}_{oc}, \boldsymbol{z}_{sc}\right) = \begin{cases} \ln\left(\boldsymbol{z}_{oc} - \boldsymbol{z}_{sc}\right) & \text{if} \quad u = 0 \quad \text{and} \quad v = 0\,, \\ \dfrac{-(u+v-1)!}{u!\,v!\left(\boldsymbol{z}_{oc} - \boldsymbol{z}_{sc}\right)^{u+v}} & \text{if} \quad u \neq 0 \quad \text{or} \quad v \neq 0\,. \end{cases} \tag{16}$$

In practice, the multipole expansion (14) must be truncated by considering $0 \leq u \leq p$ and $0 \leq v \leq p$, where the truncation number p is sufficiently large to limit the error to a prescribed value ε:

$$\left|\ln r - \Re\left(\sum_{u=0}^{p}\sum_{v=0}^{p} \mathcal{D}_u\left(\boldsymbol{z}_o, \boldsymbol{z}_{oc}\right) \mathcal{T}_{u,v}\left(\boldsymbol{z}_{oc}, \boldsymbol{z}_{sc}\right) \mathcal{A}_v\left(\boldsymbol{z}_{sc}, \boldsymbol{z}_s\right)\right)\right| < \varepsilon. \tag{17}$$

In [7], the truncation number is taken by $p = \log_2(1/\varepsilon)$. However, as will be shown, if the distance between the source point and its group center and the distance between the observation point and its group center are small compared to the distance d between the two group centers, a smaller number of terms suffices. A more economic law takes those distances into account. Let us denote by R_s the maximum distance between a source point in a source group and its center, and by R_o the maximum distance between an observation point in an observation group and its center (see Fig. 1). The value of p as a function of R_o/d and R_s/d for $\varepsilon = 10^{-6}$ and $\varepsilon = 10^{-9}$ is depicted in Fig. 2. It can be seen that in both cases $p = \log_2(1/\varepsilon)$ corresponds to $R_o/d = R_s/d = 0.35$.

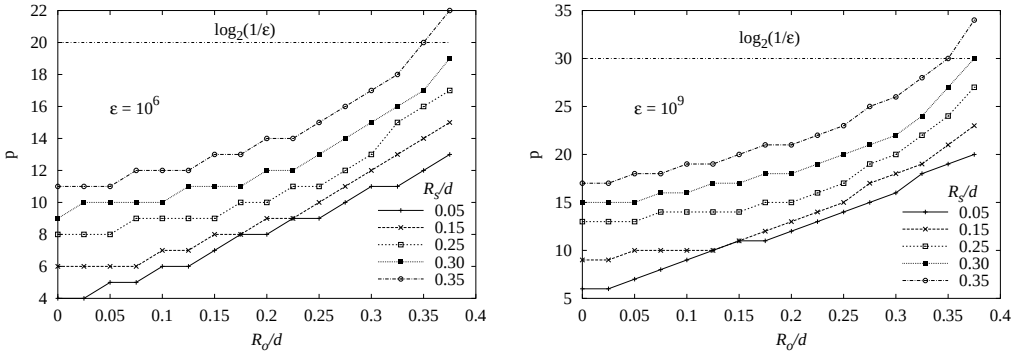

Fig. 2. Truncation number $p(R_o/d, R_s/d)$ for $\varepsilon = 10^{-6}$ (left) and $\varepsilon = 10^{-9}$ (right)

In order to apply the FMM to (10), the expansion of $\operatorname{grad} G$ is necessary as well. It can be straightforwardly obtained by deriving (15a) with respect to the coordinates of the observation point. The process to follow is then analogous.

3.2 Application of the FMM

Two groups Γ_s and Γ_o are said to be 'far groups' if $R_s/d < \tau$ and $R_o/d < \tau$, where d is the distance between the group centers and where $\tau < 1/2$.

The approximation of the matrix $\boldsymbol{M}$ can be formally written as

$$\boldsymbol{M} \;\approx\; \boldsymbol{M}^{near} + \boldsymbol{M}^{far} \;=\; \boldsymbol{M}^{near} + \underbrace{\sum_{o=1}^{\#g} \sum_{s=1}^{\#g}}_{\Gamma_o,\,\Gamma_s \text{ far}} \boldsymbol{M}^{far}_{o,s} \tag{18}$$

and analogously for the matrix $\boldsymbol{C}$.

Let us consider the degrees of freedom q_k and q_l of $q(\xi)$ with associated basis functions $\beta_k(\xi)$ and $\beta_l(\xi)$ that are nonzero on the respective far groups Γ_o and Γ_s. Substituting (14) in (11), the contribution to the corresponding element in $\boldsymbol{M}^{far}$ is given by

$$\left(\boldsymbol{M}^{far}_{o,s}\right)_{k,l} = \;\Re\left(\sum_{u=0}^{p} \boldsymbol{M}^{\mathcal{D}}_{o,k,u} \sum_{v=0}^{p} \boldsymbol{M}^{\mathcal{T}}_{u,v}\, \boldsymbol{M}^{\mathcal{A}}_{s,l,v} \right), \tag{19}$$

with

$$\boldsymbol{M}^{\mathcal{D}}_{o,k,u} = \int_{\Gamma_o} \beta_k \mathcal{D}_u\left(\boldsymbol{z}_{c_o}, \boldsymbol{z}\right) \mathrm{d}\Gamma \quad , \quad \boldsymbol{M}^{\mathcal{A}}_{s,l,v} = \int_{\Gamma_s} \beta_l \mathcal{A}_v\left(\boldsymbol{z}_{c_s}, \boldsymbol{z}\right) \mathrm{d}\Gamma\,, \tag{20}$$

$$\text{and} \;\; \boldsymbol{M}^{\mathcal{T}}_{u,v} = -\frac{1}{2\pi\nu_0} \mathcal{T}_{u,v}\left(\boldsymbol{z}_{c_o}, \boldsymbol{z}_{c_s}\right)\,. \tag{21}$$

In case of straight line elements and piecewise constant basis functions, the integrals in (20-21) can be evaluated analytically considering

$$\int_{z_1}^{z_2} \left(\boldsymbol{z}_c - \boldsymbol{z}\right)^u \mathrm{d}\boldsymbol{z} \;=\; \frac{\left(\boldsymbol{z}_c - \boldsymbol{z}_1\right)^{u+1} - \left(\boldsymbol{z}_c - \boldsymbol{z}_2\right)^{u+1}}{u+1}\,. \tag{22}$$

The assembly stage of the FMM consists in calculating and storing the required complex numbers $\boldsymbol{M}^{\mathcal{D}}_{o,k,u}$, $\boldsymbol{M}^{\mathcal{T}}_{u,v}$ and $\boldsymbol{M}^{\mathcal{A}}_{s,l,v}$. The matrix $\boldsymbol{M}^{far}$ itself is never built. The matrix $\boldsymbol{M}^{near}$ is calculated in the conventional way and stored using a sparse storage scheme.

The aim of the formal decomposition (19) is accelerating the multiplication of $\boldsymbol{M}^{far}$ by a trial vector $\boldsymbol{Q}$, required for the iterative solution of (8). Group by group, the field produced by the current layer in the considered group is aggregated into its center by (20b). This aggregated field is then subsequently translated to the centers of all the far groups by (21b), and finally the aggregated and translated field is disaggregated into the degrees of freedom of the far groups thanks to (20a).

The multiplication $\boldsymbol{M}^{far}\boldsymbol{Q}$ is further accelerated by means of the adaptive truncation scheme following the law $p = p(R_s/d, R_o/d, \varepsilon)$ shown in Fig. 2. For the $\boldsymbol{M}^{\mathcal{D}}$ and $\boldsymbol{M}^{\mathcal{A}}$ data of a given group, the truncation number p considered

during the FMM assembly stage is determined by its closest far group, $p = p_{max}$. For the $\boldsymbol{M}^{\mathcal{T}}$ data, the truncation number p is determined by the two groups Γ_s and Γ_o involved in the translation, $p = p_{so}$. During the iterative process, the aggregation step is carried out with $p = p_{max}$, while $p = p_{so}$ suffices for the translation and disaggregation steps.

4 Example

As an application example, we consider a simple 2D linear time harmonic eddy current problem. It comprises three conductors carrying a three-phase 50 Hz current and a thin steel plate placed above the conductors. The magnetic field is computed using both a FE model and a hybrid FE-BE model. In the hybrid model, the BE part is either accelerated by means of the FMM or not. Some results are presented and compared. A short discussion on the computational cost follows.

4.1 Model

Fig. 3a shows the three copper conductors with square cross-section (30 mm × 30 mm, $\mu = \mu_0$), in which balanced sinusoidal currents of frequency $f = 50$ Hz and r.m.s. value 2 kA are imposed. The horizontal distance between the centers of the conductors is 125 mm.

The steel plate is 1 mm thick and 1 m wide. It is placed 100 mm above the conductors. Its relative permeability $\mu_r = \mu/\mu_0$ and electrical conductivity σ are 1000 and $2\,10^6$ S/m, respectively. The penetration depth in the plate equals $1/\sqrt{\pi f \mu \sigma} = 2.82$ mm.

In the hybrid FE-BE model, the FE domain Ω comprises the steel plate and a layer of air around the plate. The three conductors constitute the domain Ω_s^{ext}. Fig. 3b shows a detail of the discretisation of Ω. The plate is discretised into four layers of triangular elements. The number of divisions along x is 500. Thanks to the three layers of air elements around the plate, the number of line segments on the BE contour Γ is reduced to 104 while retaining a large number of divisions in the plate. The air layer also allows to avoid the oscillation problem that may occur when using piecewise constant basis functions $\beta_k(\xi)$ on an air-iron interface [4]. The hybrid FE-BE discretisation yields 4316 complex unknowns for the harmonic analysis: 4212 for a and 104 for q.

In the FE model, the plate, the three conductors and a portion of the surrounding air are discretised by means of first order triangular elements. The discretisation of both the plate and the surrounding air layers coincides with the one in the hybrid model. The FE model is bounded by a ring (see Fig. 3c) to which a transformation method is applied in order to account for the free space extending to infinity [1]. On its outer boundary, the Dirichlet condition $a = 0$ is imposed. Two lines placed 0.5 m and 1 m above the plate, where the computed induction will be shown, are also depicted in Fig. 3c.

In order to allow a fair comparison of the hybrid model and the FE model with

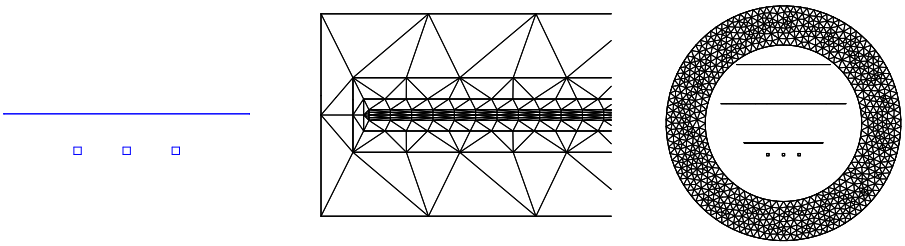

a. b. c.

Fig. 3. a. Three conductors and thin steel plate ; b. Detail of the discretisation of the domain Ω of the hybrid model ; c. Discretisation of the FE transformation domain

regard to both accuracy and computational cost, a sufficiently fine discretisation is adopted for the latter, resulting in 12844 unknowns for the harmonic analysis with a piecewise linear interpolation of the complex a.

4.2 Calculation results

The harmonic field calculations are first carried out with the FE model and the nonaccelerated hybrid FE-BE model. The flux pattern (real and imaginary part) obtained with the FE model is represented in Fig. 4.

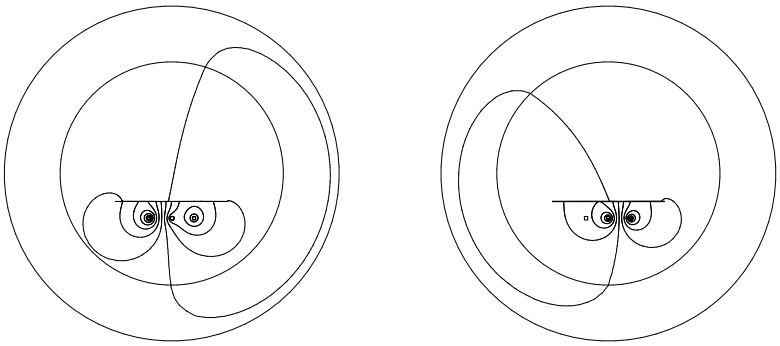

Fig. 4. Real (left) and imaginary part (right) of the flux pattern

In Fig. 5 (right) the real and imaginary part of the x-component of the magnetic induction in the four layers of the plate are depicted for both resolution methods. The agreement is very good. The discretisation of the plate in four layers proves to be necessary: due to the eddy currents, the induction is seen to vary considerably from one layer to another.

The y-component of the magnetic induction (real and imaginary part) above the plate at the distances of 0.5 m and 1.0 m is depicted in Fig. 5 (left). As expected, the curves achieved with the hybrid model are smoother and more accurate due to the fact that in the BE formulation free space is automatically and exactly considered, while in the FE model the surrounded air is discretised and a transformation method is used to account for its extension to infinity.

The FMM is now applied to speed up the BE part of the hybrid model. The BE contour Γ is split up in 25 groups constituted by either 10 line segments (the two groups on the left and right edge of the plate) or 8 line segments (the rest

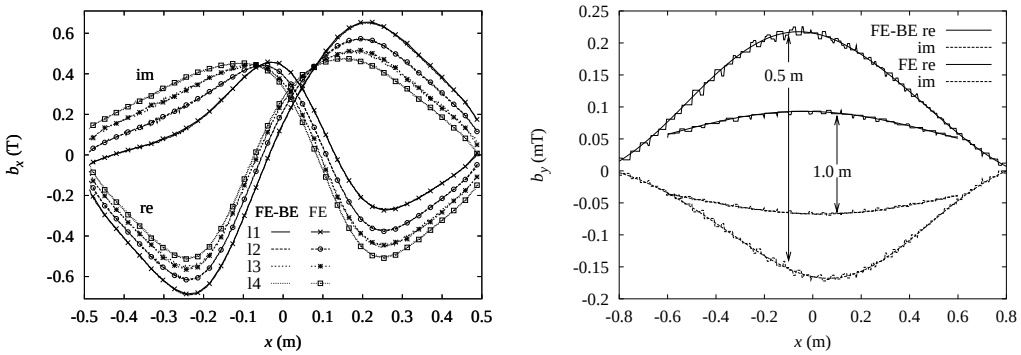

Fig. 5. Induction b_x in the four layers (denoted l1, l2, l3, l4) in which the steel plate is discretised (left) and induction b_y 0.5 m and 1.0 m above the plate (right)

of the groups). Two groups are considered to be far groups if there are at least two groups in between. This corresponds to $R_s/d \leq 1/6$ and $R_o/d \leq 1/6$, or, according to Fig. 2, to a maximum truncation number $p_{max} = 8$ for $\varepsilon = 10^{-6}$. The classical law $p = \log_2(1/\varepsilon)$ leads to a truncation number of 20.

The error of the induction in and above the plate obtained with the accelerated FE-BE hybrid model with respect to the nonaccelerated model is illustrated in Fig. 6. It is lower than 0.3% in the plate, 0.06% at 0.5 m above the plate and 0.033% at 1.0 m above the plate.

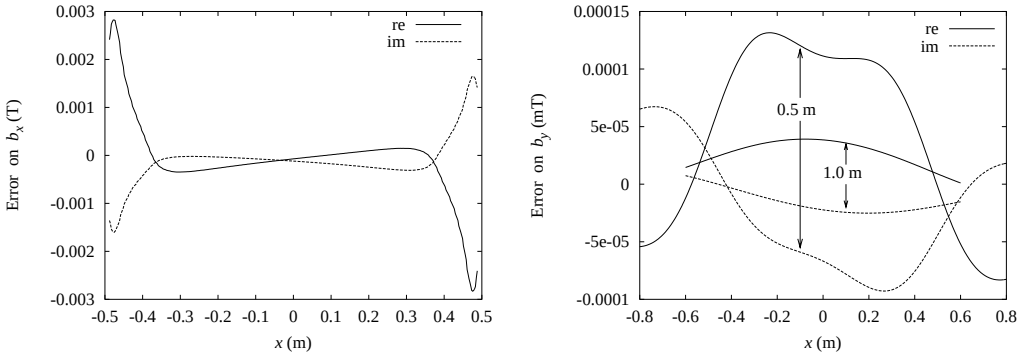

Fig. 6. Error on the induction b_x in the steel plate (left) and the induction b_y 0.5 m and 1.0 m above the steel plate (right), due to the FMM acceleration

4.3 Computational cost

For all computations, the system of algebraic equations is solved by means of the iterative solver GMRES [8]. To ensure convergence, an ILU-preconditioner is applied. In case of FMM acceleration, the ILU decomposition is based on the sparse matrix due to the FE part and the BE near-field interactions.

The total computation time on a 400 MHz MIPS R12000 Processor is 6.2 s for the FE model and 15.2 s for hybrid model without FMM acceleration. Using the FMM with the adaptive truncation scheme ($p_{max} = 8$) results in a calculation time of 9.5 s. This is mainly due to the reduced time for assembly

(8.9 s vs. 14.2 s), which constitutes in both hybrid cases approximately 93% of the total computation time. When using a fixed truncation number $p = 20$, the application of the FMM to the hybrid model does not prove useful: the computation time increases to 16.3 s.

The time spent on the iterative resolution of the system of algebraic equations is 3.8 s for the FE model and only 0.6 s for the accelerated hybrid model.

5 Conclusions

The resolution of a 2D eddy current problem by means of a hybrid FE-BE model accelerated with the FMM has been elaborated. An adaptive truncation scheme for the expansion of the 2D Laplace Green function has been envisaged. The proposed accelerated hybrid method has been successfully applied to a moderate sized test case, obtaining significant savings in the computational time.

The hybrid modelling is particularly attractive for nonlinear problems and problems with movement. Indeed, in the former case, the BE assembly needs to be done only once prior to the iterative solution by means of e.g. the Newton-Raphson method, while in the latter case, only a partial BE reassembly is required for every new position of the moving bodies. Future research will therefore focus on the accelerated hybrid modelling of such problems.

References

[1] X. Brunotte, G. Meunier, J.-F. Imhoff, Finite element modeling of unbounded problems using transformations : a rigorous, powerful and easy solution, *IEEE Transactions on Magnetics* **28** (1992) 1663–1666.

[2] A. Buchau, C. J. Huber, W. Rieger and W. M. Rucker, Fast BEM computations with the adaptive multilevel fast multipole method, *IEEE Transactions on Magnetics* **36** (2000) 680–684.

[3] J. Fetzer, S. Kurz, G. Lehner and W. M. Rucker, Analysis of an actuator with eddy currents and iron saturation: Comparison between a FEM and a BEM-FEM coupling approach, *IEEE Transactions on Magnetics* **35** (1999) 1793–1796.

[4] C. Geuzaine, T. Tarhasaari, L. Kettunen, P. Dular, Discretisation schemes for hybrid methods, *IEEE Transactions on Magnetics* **37** (2001) 3112–3115.

[5] N. Lu and J.-M. Jin, Application of fast multipole method to finite-element boundary-integral solution of scattering problems, *IEEE Transactions on Antennas and Propagation* **44** (1996) 781–786.

[6] Z. Ren, F. Bouillault, A. Razek, A. Bossavit, J.C. Vérité, A new hybrid model using electric field formulation for 3-D eddy current problems, *IEEE Transactions on Magnetics* **26** (1990) 470–473.

[7] V. Rokhlin, Rapid solution of integral equations of classical potential theory, *Journal of Computational Physics* **60** 187–207.

[8] Y. Saad and M. H. Schultz, GMRES: A Generalized Minimal Residual Algorithm for solving nonsymmetric linear systems, *SIAM J. Sci. Comput.* **7** (1986) 856–869.

[9] J. M. Song and W. C. Chew, Multilevel fast-multipole algorithm for solving combined field integral equations of electromagnetic scattering, *Micr. Opt. Tech. Lett.* **10** (1995) 14–19.